The Japan Society of Applied Physics

REGULAR PAPERS

Using aligned poly(3-hexylthiophene)/poly(methyl methacrylate) blend fibers to detect volatile organic compounds

View the article online for updates and enhancements.

Related content

REGULAR PAPER

Using aligned poly(3-hexylthiophene)/poly(methyl methacrylate) blend fibers to detect volatile organic compounds

Shun-Hsiang Chan[1†], Tz-Feng Lin[2†], Ming-Chung Wu[1,3,4*], Shih-Hsuan Chen[1], Wei-Fang Su[5], and Chao-Sung Lai[6,7,8,9]

[1]Department of Chemical and Materials Engineering, Chang Gung University, Taoyuan 33302, Taiwan
[2]3D Printing Medical Research Center, China Medical University Hospital, Taichung 40447, Taiwan
[3]Green Technology Research Center, Chang Gung University, Taoyuan 33302, Taiwan
[4]Division of Neonatology, Department of Pediatrics, Chang Gung Memorial Hospital, Linkou, Taoyuan 33305, Taiwan
[5]Department of Materials Science and Engineering, National Taiwan University, Taipei 10617, Taiwan
[6]Department of Electronic Engineering, Chang Gung University, Taoyuan 33302, Taiwan
[7]Biosensor Group, Biomedical Engineering Research Center, Chang Gung University, Taoyuan 33302, Taiwan
[8]Department of Nephrology, Chang Gung Memorial Hospital, Linkou, Taoyuan 33305, Taiwan
[9]Department of Materials Engineering, Ming Chi University of Technology, New Taipei City 24301, Taiwan

*E-mail: mingchungwu@mail.cgu.edu.tw
†These authors contributed equally to this work.

In this study, we developed a novel sensing material fabricated using a poly(3-hexylthiophene) (P3HT)/poly(methyl methacrylate) (PMMA) blend fiber on a glass substrate. The sensing materials can easily be used for sensing toluene vapor detected from extinction spectral changes. The extinction spectra variation is noted from the absorption of volatile organic compounds in a highly specific surface area of fibrous coating. An electrospinning technique is applied to generate a nonwoven structure and uniaxial orientation by fibrous coating. The response of the uniaxially orientated fibrous film is even improved at several toluene vapor concentrations. The best detection limit of this well-aligned fibrous film is up to 200 ppm for toluene vapor. © 2018 The Japan Society of Applied Physics

1. Introduction

Volatile organic compounds (VOCs) are dangerous due to their high vapor pressure at room temperature. They may pose potential risks for long-term infrastructures.[1–3] When the concentrations of VOCs are over the explosion limit, a tiny spark would trigger a serious explosion resulting in serious injury, considerable wealth loss, and death. Kaohsiung, the second-largest city in Taiwan, was ripped apart in the midnight of 31 July 2014 by a series of explosions that killed 32 people and injured at least hundreds. The blasts arose from the leaks of underground hydrocarbon chemicals. The explosion ripples overturned cars and trucks, and sent flames leaping into the downtown area.[4] It is urgent to develop safe guards for living environments and establish precaution systems beforehand. Also, accumulated chemicals could cause diseases or cancers.[5,6] If the leakage of VOCs can be detected, chronic accumulation can be avoided. One of the solutions is to develop reliable VOC sensors for public safety.

VOCs sensors are composed of chemical and physical structures for sensing materials. Table SI in the online supplementary data at http://stacks.iop.org/JJAP/57/04FM06/mmedia shows a list of the state-of-the-art research studies on VOC sensors.[1,7–13] Among VOC sensors, nanostructured sensing materials have been adopted to achieve rapid responses/high sensitivity owing to their large surface area. In contrast, the versatile electrospinning technique is a simple method that is applicable to various materials for the generation of relatively large-scale continuous electrospun fibers.[13–18]

In our previous work, we fabricated a film as a sensing material with randomly collected poly(3-hexylthiophene) (P3HT)/poly(methyl methacrylate) (PMMA) electrospun fibers. The P3HT/PMMA fibrous film exhibited acceptable sensing capability for VOCs and repeatability. The minimal
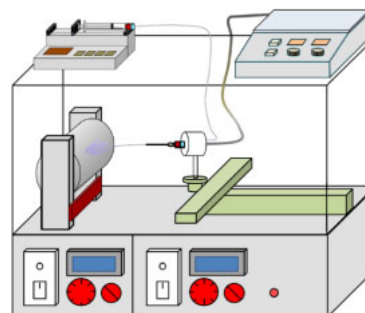
Fig. 1. (Color online) Schematic diagram of electrospinning system.

detectable concentration of 500 ppm is achieved for acetone, toluene and, *o*-xylene.[13] Herein, the aligned P3HT/PMMA fibrous film was also fabricated by electrospinning. The stacked aligned electrospun P3HT/PMMA fibrous film showed the preferred uniaxial orientation.[19]

2. Experimental procedure

PMMA (MW ∼ 996,000 Da, Aldrich) was used as received without any further purification. P3HT (MW ∼ 60,000 Da) was synthesized as described in the literature with slight modifications.[20] The P3HT solution was prepared by dissolving P3HT powder in chlorobenzene (CB; 99.8%, Acros) with continuous stirring at 40 °C for 48 h. Then, the P3HT solution was added to the stirred solution of PMMA in chlorobenzene. The P3HT/PMMA blending ratio is set at 5.0 wt % as an optimal blending ratio. The concentration of P3HT/PMMA blending solution is 15.0 wt % for electrospinning and 8.0 wt % for spin coating.

The electrospinning system (Fig. 1) includes the high-voltage power supply (Falco Tech Enterprise FES-COS), the syringe pump (KD Scientific KDS-100), and a grounded rotary collector. The maximum voltage of the voltage power
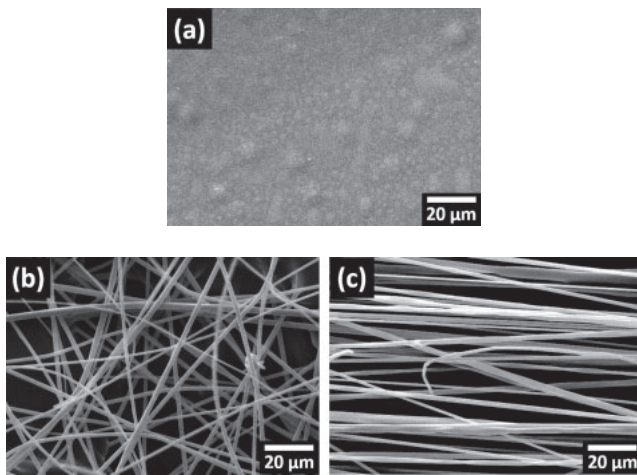
Fig. 2. SEM images of (a) P3HT/PMMA film, (b) random, and (c) aligned P3HT/PMMA blend fibers.

Fig. 3. (Color online) Extinction spectra of P3HT/PMMA film and random and aligned P3HT/PMMA fibrous films.

supply is 50.0 kV. The syringe pump automatically controls the flow rate and volume of a solution. After optimizing the applied voltage, tip-to-collector distance, the rotational speed of the rotary collector, P3HT/PMMA solution flow rate for electrospinning, and P3HT/PMMA blend fibers were prepared successfully on a glass substrate. In this study, operating parameters are fine-tuned as follows: high applied voltage is 15.0 kV; the tip-to-collector distance is fixed at 7.0 cm; the rotational speed of the rotary collector is 650 rpm; and the constant flow rate is fixed at 0.5 ml/h. In contrast, P3HT/PMMA thin films were fabricated by a spin coating at 500 rpm for 30 s. The microstructures of sensing materials with various P3HT/PMMA fibers were observed by scanning electron microscopy (SEM; SEC SNE-4500M) operated at an accelerating voltage of 15.0 kV. To sense toluene vapor at a saturated vapor pressure, excess toluene liquid was added into an enclosed 80 mL quartz container with the P3HT/PMMA fibrous film at the center of the container. Moreover, for sensing low-concentration toluene vapor, several controlled amounts of toluene liquid was added into the same container individually; thus, a controlled vapor concentration was obtained after the liquid VOCs completely evaporated within the quartz bottle. An ultraviolet–visible spectrometer (JASCO V-730) was utilized to measure the extinction spectra of the P3HT/PMMA-sensing materials.

3. Results and discussion

Three kinds of 5.0 wt % P3HT/PMMA-sensing materials were fabricated by spin coating and electrospinning. For the spin coated sensing material, the P3HT/PMMA film shows obvious phase separation in a SEM image in Fig. 2(a). P3HT island like domains are formed owing to the poor solubility of P3HT in PMMA.[21,22] The optimized parameters for electrospinning were set to prepare specimens as follows: an applied voltage of 15.0 kV, a tip-to-collector distance of 7.0 cm, a rotary collector rotational speed of 650 rpm, and a solution flow rate of 0.5 ml/h. SEM images of random and aligned P3HT/PMMA blend fibers are shown in Figs. 2(b) and 2(c). The aligned P3HT/PMMA fibrous film exhibits the preferred uniaxial orientation in contrast to the random orientation. The average diameter of random and aligned P3HT/PMMA blend fibers is $1.39 \pm 0.01 \mu m$.
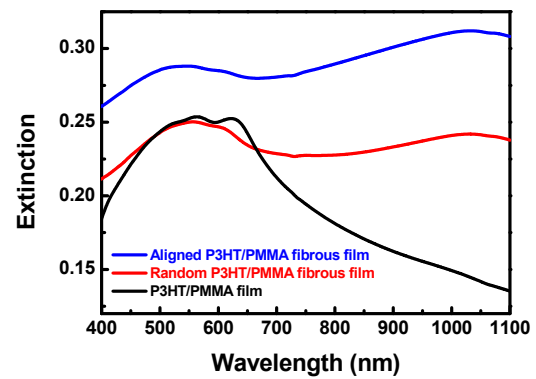
Figure 3 shows the UV–vis extinction spectra of the P3HT/PMMA film and the random, and aligned P3HT/PMMA fibrous films. The extinction spectra of the P3HT/PMMA film exhibit the λ_{max} at 560 nm and pronounced 0–0 and 0–1 vibronic extinction peaks at 600 nm.[23–25] The extinction spectra of the random P3HT/PMMA fibrous film also show the peaks at 560 and 600 nm. In particular, it is note worthy that the peak intensity at 1,020 nm is increased. It is more obvious for the aligned P3HT/PMMA fibrous film than for the random P3HT/PMMA fibrous film. We speculate that the extra peak at 1,020 nm observed in the fibrous sample only is due to light scattering. The literature indicated that the preferred uniaxial orientation could enhance optical properties.[26,27] The significant changes in extinction spectra were found after the exposure of the P3HT/PMMA fibrous film to VOCs.

To ensure the sensing capability of several P3HT/PMMA-sensing materials, toluene vapor is used in the VOC test for 120 min. Toluene is extensively used as an industrial feedstock and a solvent. In addition, we define the response, R, of a fibrous film according to the extinction spectra variation at two distinguished wavelengths of 600 and 1,020 nm. The equations of R for fibrous films at 600 and 1,020 nm are

$$R_{600} = \frac{E_{t(600)} - E_{0(600)}}{E_{0(600)}} \qquad (1)$$

$$R_{1020} = \frac{E_{t(1020)} - E_{0(1020)}}{E_{0(1020)}} \qquad (2)$$

where $E_{o(x)}$ is the extinction without VOC exposure (i.e., 0 min); $E_{t(x)}$ is the recorded extinction with respect to toluene vapor exposure time.

The detection capability of the three P3HT/PMMA-sensing materials are shown in Fig. 4. The extinction spectra [Fig. 4(a)] and responses [Fig. 4(b)] of P3HT/PMMA films show no significant difference under saturated toluene vapor. These results indicate that a flat film could not adsorb toluene vapor at all; thus, the spectra show no differences. When the random P3HT/PMMA fibrous film is exposed to saturated toluene vapor, the response curves [Fig. 4(d)] show three stages involved in toluene vapor sensing.[13] In the first stage, toluene is adsorbed on the surface of the fibrous film. In the second stage, the fibrous film starts to collapse. In the last stage, the collapsed fibrous film continuously adsorbs VOCs and becomes swelled by VOCs, the scattering effect of the
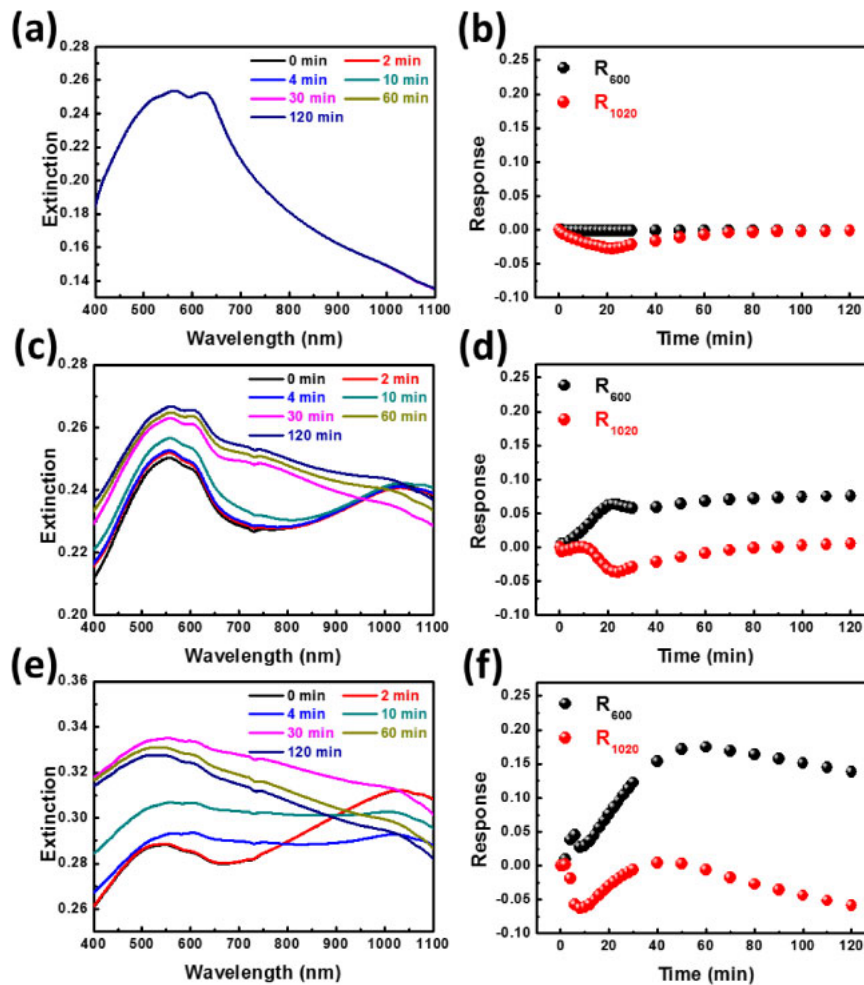
Fig. 4. (Color online) Extinction spectra and responses of (a, b) P3HT/PMMA film and (c, d) random and (e, f) aligned P3HT/PMMA fibrous films exposed to saturated toluene for different times.

microstructures disappeared [Fig. 4(c)]. Similarly, according to published reports, a film with preferred uniaxial orientation was used to modulate optical behavior.[26–28] The propagation of light was regulated by restricting its emission directions at certain frequencies or localizing light in specific areas. Results suggest that the well-aligned $\sim$1.39 μm P3HT/PMMA fibers strongly scatters the light at 1,020 nm. R_{1020} would thus show noticeable variations in our fibers. The extinction spectra of the sensing material with aligned P3HT/PMMA fibers exposed to saturated toluene vapor for different times, show the larger variation than the other two sensing materials [Fig. 4(e)]. The response of various sensing materials exposed to saturated toluene vapor for different times is shown in Figs. 4(b), 4(d), and 4(f). The sensing material with aligned P3HT/PMMA fibers exhibited the largest extinction variation and definitely the highest responsivity among all the sensing materials [Fig. 4(f)].

Most importantly, the responses of three kinds of P3HT/PMMA-sensing materials exposed to low-concentration toluene vapor were measured as shown in Fig. 5. The toluene vapor concentrations are individually set at 10,000, 2,000, 500, and 200 ppm. The response time is defined as the time at a fixed toluene vapor concentration at which the P3HT/PMMA-sensing materials give responses larger than two times of the sensing error ($\sim$0.002). The sensing material

with aligned P3HT/PMMA fibers always exhibited the highest responsivity among the three sensing materials. The detection limits of the P3HT/PMMA film and random and aligned P3HT/PMMA fibrous films exposed to four concentrations of toluene vapor is summarized in Table I. For detecting toluene vapor at concentrations of 10,000, 2000, and 500 ppm, the response times of the aligned P3HT/PMMA fibrous film are all less than 16 min. Regarding a nonwoven structure, the preferred uniaxial orientation could enhance the extinction changes following VOC exposure. Moreover, the aligned P3HT/PMMA fibrous film is further more sensitive to 200 ppm toluene vapor. The detection resolution for the P3HT/PMMA fibrous film is much lower than the lower explosive limit (LEL) of toluene (12,000 ppm).[29] We suggest the aligned P3HT/PMMA fibrous film can be applied well to toluene-related derivatives.

4.   Conclusions

P3HT/PMMA-sensing materials were fabricated successfully by electrospinning. The sensing material fabricated from aligned fibrous P3HT/PMMA on a glass substrate has shown an excellent response to toluene at 500 ppm and a rapid-response time of 16 min. The detection limit achieved for toluene vapor is 200 ppm. This low-cost and fast-responding VOC sensor extends the current VOC sensing technology.
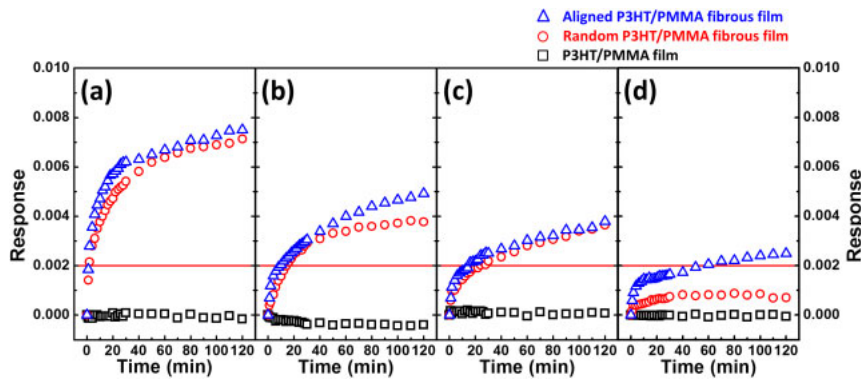
Fig. 5. (Color online) R_{600} of P3HT/PMMA film and random and aligned P3HT/PMMA fibrous films exposed to toluene vapor at different concentrations, including (a) 10,000, (b) 2,000, (c) 500, and (d) 200 ppm.

Table I. Response times (min) of P3HT/PMMA film and random and aligned P3HT/PMMA fibrous films exposed to toluene vapor at four concentrations.

	Concentration (ppm)			
	10,000	2,000	500	200
P3HT/PMMA film	N/A	N/A	N/A	N/A
Random P3HT/PMMA fiber	2	16	24	N/A
Aligned P3HT/PMMA fiber	2	10	16	60

1) H. Guo, A. Guo, Y. Gao, and T. Liu, Sensors **17**, 1764 (2017).
2) Y. Zhang, J. Zhao, T. Du, Z. Zhu, J. Zhang, and Q. Liu, Sci. Rep. **7**, 1960 (2017).
3) A. Schütze, T. Baur, M. Leidinger, W. Reimringer, R. Jung, T. Conrad, and T. Sauerwald, Environments **4**, 20 (2017).
4) CNN News [http://edition.cnn.com/2014/07/31/world/asia/taiwan-explosions/index.html].
5) G. St. Helen, P. Jacob, III, M. Peng, D. A. Dempsey, S. K. Hammond, and N. L. Benowitz, Cancer Epidemiol. Biomarkers Prev. **23**, 2774 (2014).
6) P. Williams, L. Benton, J. Warmerdam, and P. Sheehan, Environ. Sci. Technol. **36**, 4721 (2002).
7) A. Kösemen, S. Öztürk, Z. Şen, Z. A. Kösemen, M. Harbeck, and Z. Ziya Öztürk, J. Electrochem. Soc. **164**, B657 (2017).

8) J. Baek, D. Yin, N. Liu, I. Omkaram, C. Jung, H. Im, S. Hong, S. M. Kim, Y. K. Hong, J. Hur, Y. Yoon, and S. Kim, Nano Res. **10**, 1861 (2017).
9) T. Kida, K. Suematsu, K. Hara, K. Kanie, and A. Muramatsu, ACS Appl. Mater. Interfaces **8**, 35485 (2016).
10) S.-Y. Cho, H.-J. Koh, H.-W. Yoo, J.-S. Kim, and H.-T. Jung, ACS Sens. **2**, 183 (2017).
11) Y. Gao, Q. Kong, J. Zhang, and G. Xi, RSC Adv. **7**, 35897 (2017).
12) H.-C. Liao, C.-P. Hsu, M.-C. Wu, C.-F. Lu, and W.-F. Su, Anal. Chem. **85**, 9305 (2013).
13) M.-C. Wu, S.-H. Chan, T.-F. Lin, C.-F. Lu, and W.-F. Su, J. Taiwan Inst. Chem. Eng. **78**, 552 (2017).
14) K. Azuma, K. Sakajiri, T. Okabe, H. Matsumoto, S. Kang, J. Watanabe, and M. Tokita, Jpn. J. Appl. Phys. **56**, 095002 (2017).
15) T. Q. Duong, H. Kobayashi, Y. Inoue, and H. Moritake, Jpn. J. Appl. Phys. **56**, 061701 (2017).
16) Y. Horie, M. Deguchi, S. Guo, K. Aoki, and T. Nomiyama, Jpn. J. Appl. Phys. **53**, 05FB01 (2014).
17) C. J. Ge and J. N. Choi, Nanomaterials **7**, 60 (2017).
18) H. Du, P. Yao, Y. Sun, J. Wang, H. Wang, and N. Yu, Sensors **17**, 1822 (2017).
19) S.-H. Chan, M.-C. Wu, S.-H. Chen, W.-F. Su, and C.-S. Lai, Int. Conf. Solid State Devices and Materials, 2017, PS-11-09.
20) R. S. Loewe, P. C. Ewbank, J. Liu, L. Zhai, and R. D. McCullough, Macromolecules **34**, 4324 (2001).
21) M.-C. Wu, H.-C. Liao, Y. Chou, C.-P. Hsu, W.-C. Yen, C.-M. Chuang, Y.-Y. Lin, C.-W. Chen, Y.-F. Chen, and W.-F. Su, J. Phys. Chem. B **114**, 10277 (2010).
22) L. Kergoat, N. Battaglini, L. Miozzo, B. Piro, M.-C. Pham, A. Yassar, and G. Horowitz, Org. Electron. **12**, 1253 (2011).
23) V. Vohra, F. Galeotti, U. Giovanella, T. Anzai, E. Kozma, and C. Botta, Appl. Phys. Lett. **109**, 103702 (2016).
24) A. Thiessen, J. Vogelsang, T. Adachi, F. Steiner, D. Vanden Bout, and J. M. Lupton, Proc. Natl. Acad. Sci. U.S.A. **110**, E3550 (2013).
25) O. P. Dimitriev, Nanoscale Res. Lett. **12**, 510 (2017).
26) O. Matsumoto, K. Miura, H. Kawaguchi, M. Sano, M. Saito, Y. Hirano, W. Kada, and O. Hanaizumi, Results Phys. **7**, 2965 (2017).
27) M. Imanishi, D. Kajiya, T. Koganezawa, and K.-I. Saitow, Sci. Rep. **7**, 5141 (2017).
28) T. Nobeshima, H. Sakai, Y. Ishii, S. Uemura, and M. Yoshida, J. Photopolym. Sci. Technol. **29**, 353 (2016).
29) Web [https://www.mathesongas.com/pdfs/products/Lower-(LEL)-&-Upper-(UEL)-Explosive-Limits-.pdf].